

Fluorene-Based Conjugated Copolymers Containing Hexyl-Thiophene Derivatives for Organic Thin Film Transistors[†]

Hoyoul Kong, Dae Sung Chung,[‡] In-Nam Kang,[§] Eunhee Lim,[#] Young Kwan Jung,
Jong-Hwa Park, Chan Eon Park,^{‡,*} and Hong-Ku Shim^{*}

Department of Chemistry and School of Molecular Science (BK21), Korea Advanced Institute of Science and Technology, Daejeon 305-701, Korea. *E-mail: hkshim@kaist.ac.kr

[‡]Polymer Research Institute, Department of Chemical Engineering, Pohang University of Science and Technology, Pohang 790-784, Korea. *E-mail: cep@postech.ac.kr

[§]Department of Chemistry, The Catholic University of Korea, Bucheon, Gyeonggi 420-743, Korea

[#]Melville Laboratory for Polymer Synthesis, Department of Chemistry, University of Cambridge, Lensfield Road, Cambridge CB2 1EW, UK

Received June 25, 2007

Two fluorene-based conjugated copolymers containing hexyl-thiophene derivatives, PF-1T and PF-4T, were synthesized *via* the palladium-catalyzed Suzuki coupling reaction. The number-average molecular weights (M_n) of PF-1T and PF-4T were found to be 19,100 and 13,200, respectively. These polymers were soluble in common organic solvents such as chloroform, chlorobenzene, toluene, etc. The UV-vis absorption maximum peaks of PF-1T and PF-4T in the film state were found to be 410 nm and 431 nm, respectively. Electrochemical characterization revealed that these polymers have low highest occupied molecular orbital (HOMO) levels, indicating good resistance against oxidative doping. Thin film transistor devices were fabricated using the top contact geometry. PF-1T showed much better thin-film transistor performance than PF-4T. A thin film of PF-1T gave a saturation mobility of 0.001–0.003 cm² V⁻¹ s⁻¹, an on/off ratio of 1.0×10^5 , and a small threshold voltage of –8.3 V. To support TFT performance, we carried out DSC, AFM, and XRD measurements.

Key Words : Fluorene, Thiophene, Organic thin-film transistor (OTFT)

Introduction

Conjugated polymers have attracted considerable attention for various applications, including light-emitting diodes (OLEDs),^{1–3} thin-film transistors (TFTs),^{4–6} and photovoltaic cells (PVs).^{7–9} Among these organic electronic devices, organic TFTs can be used in low cost memories, smart cards, and the driving circuits of large-area display devices.^{10–12} To enable low-cost manufacturing, it is preferable to be fabricated TFTs using simple solution techniques under ambient conditions. However, many solution-processable semiconducting polymers showed poor TFT performances including low mobility and low current on/off ratio when the TFT devices were fabricated in ambient conditions. To solve these problems, it is important to design and synthesize organic semiconductors with good resistance against atmospheric oxygen doping. The oxidative doping of semiconducting conjugated polymers depends on their ionization potentials (IPs), *i.e.*, their highest occupied molecular orbital (HOMO) levels from vacuum.¹³ Therefore, to reduce oxidative doping, semiconducting materials must have low HOMO levels. Recently, new semiconducting polymers with low HOMO levels and good ordering from side alkyl chains have been reported.^{13–15}

In this paper, we report solution-processable fluorene-

based copolymers containing hexyl-thiophene derivatives in the main chain that can be employed to lower the HOMO levels. Especially this paper suggests very important information on the relationship between the structures of semiconducting materials and their TFT device performances by coupling hexyl-thiophene derivatives having different thiophene unit lengths.

Experimental Section

Materials. 3-Hexylthiophene, *N*-bromosuccinimide (NBS), 2-Isopropoxy-4,4,5,5-tetramethyl-1,3,2-dioxaborolane, tetrakis(triphenylphosphine)palladium, Aliquat[®] 336 were purchased from Aldrich Chemical Co. All reagents purchased commercially were used without further purification except for tetrahydrofuran (THF) dried over sodium/benzophenone.

Synthesis of the Monomers. 2,2'-(9,9-Dihexyl-9H-fluorene-2,7-diyl)bis(4,4,5,5-tetramethyl-1,3,2-dioxaborolane) was synthesized according to the literature method.¹⁶ ¹H NMR (CDCl₃, 400 MHz): δ (ppm) 7.77 (d, 2H), 7.73 (s, 2H), 7.71 (d, 2H), 1.98 (m, 4H), 1.37 (s, 24H), 0.99 (m, 12H), 0.72 (t, 6H), 0.53 (m, 4H). EIMS *m/z* 586.45. Anal. Calcd for C₃₇H₅₆B₂O₄: C, 75.78; H, 9.62. Found: C, 75.97; H, 9.86.

2-Bromo-3-hexylthiophene (1): To a solution of 3-hexylthiophene (10.0 g, 59.42 mmol) and 120 mL acetic acid, NBS (11.63 g, 65.36 mmol) was added in one portion and stirred for 30 min. And then water was added into the

[†]This paper is dedicated to professor Sang Chul Shim on the occasion of his honorable retirement.

resulting solution, and also stirred for 10 min. The mixture was washed with ether, saturated aqueous NaHCO₃, and water, and dried with MgSO₄. The solvent was removed *via* rotary evaporation, and 2-bromo-3-hexylthiophene (12.54 g, 86%) was obtained. ¹H NMR (CDCl₃, 400 MHz): δ (ppm) 7.17 (d, 1H), 6.80 (d, 1H), 2.59 (t, 2H), 1.60 (m, 2H), 1.35 (m, 6H), 0.93 (t, 3H).

2,5-Dibromo-3-hexylthiophene (2): To a stirred solution of 2-bromo-3-hexylthiophene (1) (4.0 g, 16.18 mmol) in chloroform and acetic acid (120 mL, 1:1 v/v), NBS (5.76 g, 32.36 mmol) was added, and mixture was refluxed for 1.5 h. Water was added, and the organic layer was extracted with chloroform, washed with 2.0 M KOH, and dried with MgSO₄. The solvent was removed *via* rotary evaporation, and the resulting dark oil was filtered through a short pad of silica with hexanes. Removal of the solvent by rotary evaporation yielded 3.21 g (61%) of (2) as a colorless oil. ¹H NMR (CDCl₃, 400 MHz): δ (ppm) 6.77 (s, 1H), 2.51 (t, 2H), 1.54 (m, 2H), 1.33 (m, 6H), 0.91 (m, 3H). EIMS *m/z* 326.04. Anal. Calcd for C₁₀H₁₄Br₂S: C, 36.83; H, 4.33; S, 9.83. Found: C, 36.85; H, 4.38; S, 9.87.

2-(4-Hexylthiophen-2-yl)-4,4,5,5-tetramethyl-1,3,2-dioxaborolane (3): To a solution of 3-hexylthiophene (4.68 g, 27.80 mmol) in THF (50 mL) at -15 °C, 4.62 mL (30.59 mmol) of TMEDA and 17.99 mL (30.59 mmol) of tert-BuLi (1.7 M in pentane) was added, by syringe. The mixture was stirred at 60 °C for 2 h. 2-Isopropoxy-4,4,5,5-tetramethyl-1,3,2-dioxaborolane (6.24 mL, 30.59 mmol) was added to the solution, and the resulting mixture was stirred at -78 °C for 1 h and warmed to room temperature and stirred for 12 h. The mixture was poured into water, extracted with ether, dried with MgSO₄. The solvent was removed *via* rotary evaporation, and the residue was distilled. The product yield was 4.66 g (57%). ¹H NMR (CDCl₃, 400 MHz): δ (ppm) 7.48 (s, 1H), 7.20 (s, 1H), 2.62 (t, 2H), 1.63 (m, 2H), 1.30 (m, 18H), 0.89 (t, 3H).

3,4'-Dihexyl-2,2'-bithiophene (4): To a stirred mixture of 2-(4-hexylthiophen-2-yl)-4,4,5,5-tetramethyl-1,3,2-dioxaborolane (3) (6 g, 20.39 mmol), tetrakis(triphenylphosphine)palladium (0.95 g, 0.82 mmol), and Aliquat[®] 336 (0.085 g, 0.21 mmol) in 40 mL of anhydrous toluene, 2 M aqueous sodium carbonate solution (13.26 mL) was added. The solution was refluxed with vigorous stirring for 20 h under nitrogen atmosphere. The mixture was poured into water (100 mL) and extracted with ethyl acetate. The extract was successively washed water and brine. After dryness (MgSO₄), the solvent was evaporated and the residue was purified by column chromatography on silica gel with hexane to give product (6.2 g, 91%). ¹H NMR (CDCl₃, 400 MHz): δ (ppm) 7.16 (d, 1H), 6.99 (s, 1H), 6.95 (d, 1H), 6.90 (s, 1H), 2.80 (t, 2H), 2.65 (t, 2H), 1.68 (m, 4H), 1.37 (m, 12H), 0.94 (m, 6H).

5'-Bromo-3,4'-dihexyl-2,2'-bithiophene (5): 5'-Bromo-3,4'-dihexyl-2,2'-bithiophene (5) was synthesized using the same method as for compound (1) with 0.90 g of 3,4'-dihexyl-2,2'-bithiophene (4) and 0.53 g of NBS. The final product was obtained after drying, yielding 0.70 g (64%). ¹H

NMR (CDCl₃, 400 MHz): δ (ppm) 7.15 (d, 1H), 6.91 (d, 1H), 6.81 (s, 1H), 2.72 (t, 2H), 2.56 (t, 2H), 1.61 (m, 4H), 1.35 (m, 12H), 0.91 (m, 6H). ¹³C NMR (CDCl₃, 400 MHz): δ (ppm) 142.2, 139.8, 135.6, 129.9, 129.8, 126.7, 123.8, 108.4, 31.6, 31.5, 30.6, 29.6, 29.5, 29.4, 29.2, 29.1, 29.0, 28.8, 22.6, 14.0.

2-(3,4'-Dihexyl-2,2'-bithiophen-5-yl)-4,4,5,5-tetramethyl-1,3,2-dioxaborolane (6): 2-(3,4'-Dihexyl-2,2'-bithiophen-5-yl)-4,4,5,5-tetramethyl-1,3,2-dioxaborolane (6) was synthesized using the same method as for compound (3) with 2.0 g of 3,4'-dihexyl-2,2'-bithiophene (4) and 1.34 mL of 2-isopropoxy-4,4,5,5-tetramethyl-1,3,2-dioxaborolane. The final product was obtained after drying, yielding 2.13 g (77 %). ¹H NMR (CDCl₃, 400 MHz): δ (ppm) 7.43 (s, 1H), 6.97 (s, 1H), 6.87 (s, 1H), 2.74 (t, 2H), 2.61 (t, 2H), 1.59 (m, 4H), 1.30 (m, 24H), 0.85 (m, 6H).

4T (7): 4T (7) was synthesized using the same method as for compound (4) with 0.7 g of 5'-bromo-3,4'-dihexyl-2,2'-bithiophene (5) and 0.78 g of 2-(3,4'-dihexyl-2,2'-bithiophen-5-yl)-4,4,5,5-tetramethyl-1,3,2-dioxaborolane (6). The final product was obtained after drying, yielding 0.77 g (68 %). ¹H NMR (CDCl₃, 400 MHz): δ (ppm) 7.15 (d, 1H), 6.96 (m, 5H), 2.65 (m, 8H), 1.67 (m, 8H), 1.36 (m, 24H), 0.92 (m, 12H). ¹³C NMR (CDCl₃, 400 MHz): δ (ppm) 143.5, 139.6, 135.5, 133.9, 133.5, 130.9, 130.5, 130.4, 130.0, 128.6, 128.3, 127.1, 127.0, 123.4, 119.9, 119.8, 31.6, 30.6, 30.5, 30.4, 30.3, 29.4, 29.3, 29.2, 29.1, 29.0, 22.6, 14.0.

Dibromo-4T (8): To a solution of 4T (7) (0.71 g, 1.06 mmol) and 7 mL chloroform and acetic acid (1:1 v/v), NBS (0.38 g, 2.13 mmol) was added in one portion and stirred for 30 min. And then water was added into the resulting solution, and also stirred for 10 min. The mixture was washed with washed with ether, saturated aqueous NaHCO₃, and water, and dried with MgSO₄. A solvent was removed *via* rotary evaporation, and dibromo-4T (8) (0.83 g, 95%) was obtained. ¹H NMR (CDCl₃, 400 MHz): δ (ppm) 6.96 (s, 1H), 6.89 (s, 1H), 6.88 (s, 1H), 6.85 (s, 1H), 2.71 (m, 8H), 1.65 (m, 8H), 1.36 (m, 24H), 0.92 (m, 12H). EIMS *m/z* 824.37. Anal. Calcd for C₄₀H₅₆Br₂S₄: C, 58.24; H, 6.84; S, 15.55. Found: C, 58.68; H, 6.89; S, 15.96.

Polymerization. The synthesis of the copolymers was carried out using palladium-catalyzed Suzuki coupling. All starting materials, reagents, and solvents were carefully purified, and all the procedures were performed under an air-free environment. 2,2'-(9,9-dihexyl-9H-fluorene-2,7-diyl)-bis(4,4,5,5-tetramethyl-1,3,2-dioxaborolane), Pd(PPh₃)₄ (0.02 mol %), a thiophene-containing comonomer, 2,5-dibromo-3-hexylthiophene (2) or dibromo-4T (8), and several drops of Aliquat[®] 336 were dissolved in a solution of toluene and aqueous 2 M Na₂CO₃, respectively. The mixture was stirred for 3 days at 80 °C, and then bromo-benzene and phenyl boronic acid was added as end cappers in order at 6 h intervals. After additional stirring for 6 h, aqueous 2 M HCl solution was added into the mixture was poured into methanol. The resulting solids were washed with acetone to remove oligomers and other impurities.

¹H NMR (CDCl₃, 400 MHz): δ (ppm), PF-IT: 7.66 (b,

4H), 7.49 (b, 2H), 7.33 (b, 1H), 2.77 (b, 2H), 2.06 (b, 4H), 1.73 (b, 2H), 1.39 (b, 8H), 1.11 (b, 14H), 0.79 (b, 9H). PF-4T: 7.70 (b, 5H), 7.53 (b, 2H), 6.99 (b, 3H), 2.70 (b, 8H), 2.01 (b, 4H), 1.70 (b, 8H), 1.33 (b, 24H), 1.06 (b, 14H), 0.81 (b, 20H).

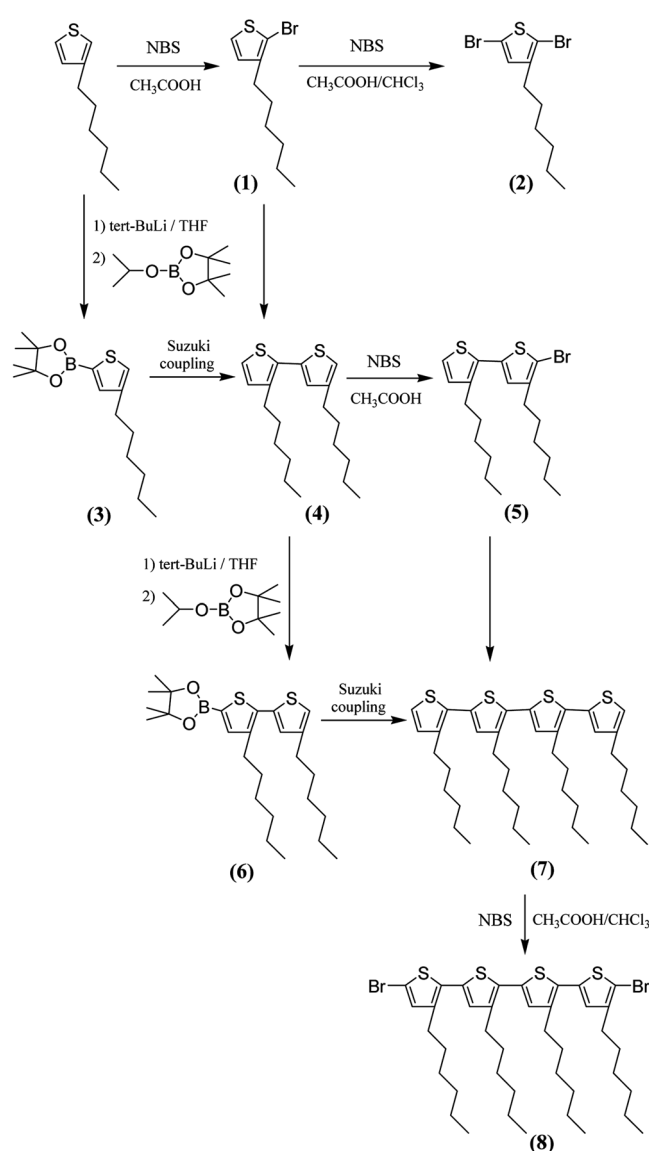
Anal. Calcd for PF-1T (C₃₅H₄₈S): C, 83.94; H, 9.66; S, 6.40. Found: C, 83.13; H, 9.31; S, 6.23. Calcd for PF-4T (C₆₅H₉₀S₄): C, 78.10; H, 9.07; S, 12.83. Found: C, 78.02; H, 8.95; S, 12.59.

Fabrication of the OTFT Devices. Thin-film transistors (TFTs) were fabricated on silicon wafer using the top contact geometry (channel length $L = 150 \mu\text{m}$, width $W = 1500 \mu\text{m}$) in ambient conditions without taking any special precautions to exclude air, moisture, and light. A heavily n-doped silicon wafer with a 300 nm thermal silicon dioxide (SiO₂) was used as the substrate/gate electrode, with the top SiO₂ layer serving as the gate dielectric. The SiO₂ surface of the wafer substrate was first cleaned with piranha solution and the cleaned wafer was immersed in a solution of octyltrichlorosilane (OTS-8) in toluene at room temperature for 2 h. The semiconductor layer was spin-coated at 2000 rpm from 0.4 wt % chloroform solution, with a thickness of 40 nm. Subsequently, a series of gold source/drain electrode pairs were deposited by vacuum evaporation through a shadow mask. Silicon oxide at the backside of the silicon wafer of the TFT device was removed with sandpaper to provide a conductive gate contact.

Results and Discussion

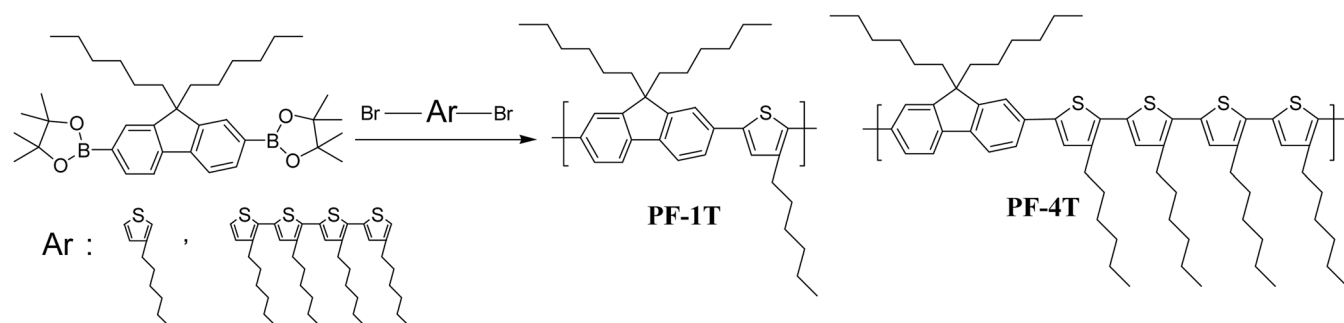
Synthesis. The synthetic routes for the monomers and polymers are shown in Schemes 1 and 2, respectively. The polymers were prepared by using the palladium-catalyzed Suzuki coupling method. The two polymers were soluble in common organic solvents such as chloroform and chlorobenzene without evidence of gel formation at room temperature. The molecular weights and polydispersity indices of the polymers were determined *via* gel permeation chromatography (GPC) using THF as the eluent and polystyrene as the standard. The number-average molecular weights (M_n) of PF-1T and PF-4T were found to be 19,100 and 13,200, with polydispersity indices of 1.98 and 2.03, respectively.

Optical and Electrochemical Properties. Figure 1 shows the normalized UV-vis absorption and photoluminescence (PL) emission spectra of the polymers in the film



Scheme 1. Synthetic routes for the monomers.

state. The UV-vis absorption maximum peaks of PF-1T and PF-4T in the film state appeared at 410 and 431 nm, respectively. The PL emission maximum peak of PF-1T in the film state appeared at 503 nm with shoulder peaks at 473 nm whereas PF-4T appeared at 577 nm. These results indicate that the effective conjugation length of PF-4T is longer than that of PF-1T in the bulk state of the film.



Scheme 2. Synthetic routes for the polymers.

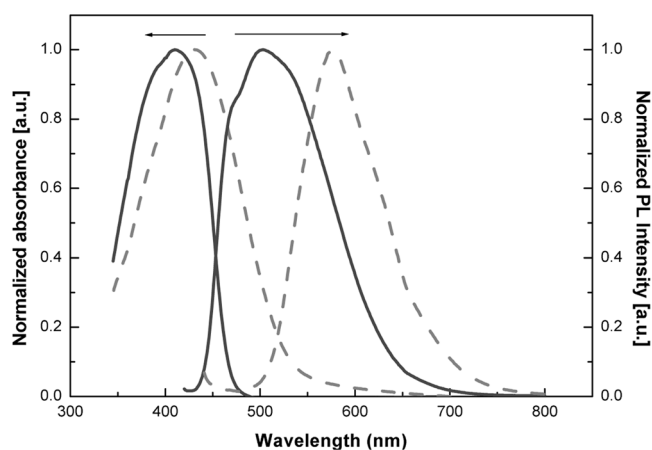


Figure 1. UV-vis absorption and PL emission spectra of PF-1T (solid line) and PF-4T (dotted line) in film form.

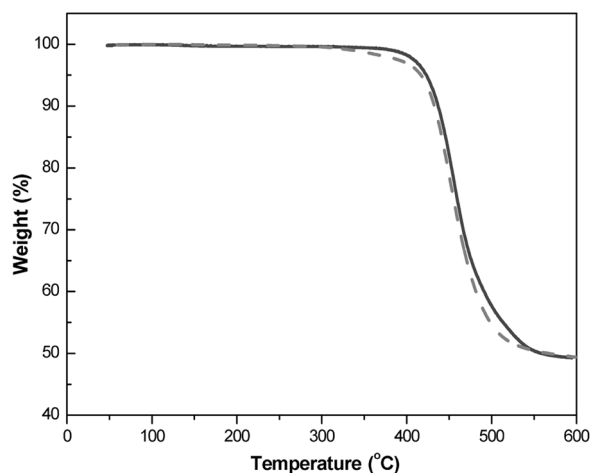


Figure 2. TGA thermograms of PF-1T (solid line) and PF-4T (dotted line).

The electrochemical behavior of the polymers was investigated using cyclic voltammetry (CV). The oxidation potential E_{OX} (p-doping) for PF-1T and PF-4T was 1.25 and 1.10 V, respectively, corresponding to HOMO levels of -5.53 and -5.38 eV, respectively (with respect to the energy level of the ferrocene reference -4.8 eV below the vacuum level).^{17,18} The ionization potential of PF-1T was 0.15 eV higher than that of PF-4T. Therefore, PF-1T has a greater resistance against oxidative doping.

Thermal and Crystalline Properties. Thermal stabilities of the polymers were investigated by thermogravimetric analysis (TGA) (see the Figure 2). The two polymers, PF-1T and PF-4T, showed very good thermal stability and did not decompose until roughly 400 °C under nitrogen atmosphere. Differential scanning calorimetry (DSC) measurements were also performed under N_2 flow, and the results are shown in Figure 3. DSC results showed that PF-1T has a phase transition at 185 °C due to backbone melting, but does not exhibit liquid crystalline (LC) phases. In the case of PF-4T, no phase transitions were shown. It is thought that PF-4T might have an amorphous structure or a transition temperature might exist above higher temperature.

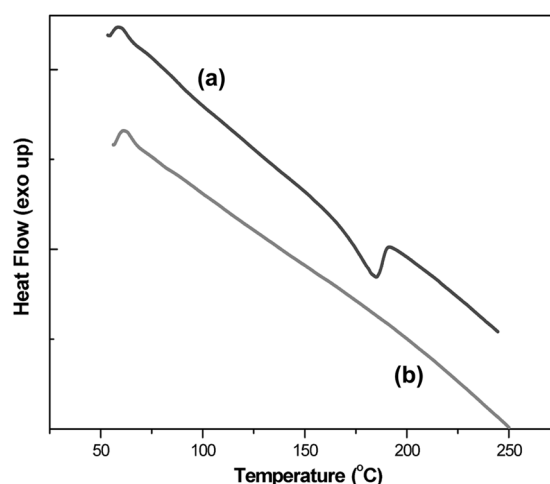


Figure 3. DSC thermogram of PF-1T (a) and PF-4T (b).

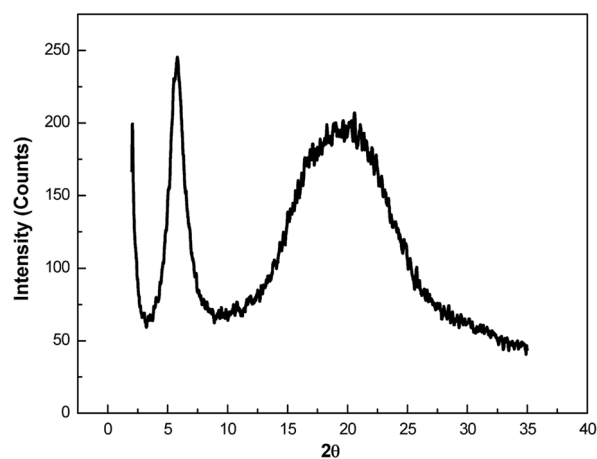


Figure 4. XRD patterns of PF-1T as a film.

Structural orderings of PF-1T in thin film were studied by X-ray diffraction (XRD). Thin film of this polymer was prepared on an OTS-8 modified substrate by drop-casting from 1 wt % polymer solution in chloroform. Out-of-plane XRD spectrum of the PF-1T is shown in Figure 4. In the XRD pattern of the film, there is a clear peak at 15.3 \AA ($2\theta = 5.8^\circ$), which corresponds to the distance governed by the hexyl-groups, and a broad peak at 4.5 \AA ($2\theta = 19.6^\circ$), which corresponds to the face-to-face distance between coplanar polymer chains. These peaks are consistent with the previously reported layer periodicities observed for alkyl-substituted fluorene- or thiophene-based polymers.¹⁹⁻²² These results suggest that the PF-1T chains are aligned to a significant extent and are separated from each other by hexyl groups that are oriented normal to the substrate to some extent. This alignment of the polymer chains is expected to enhance the performance of PF-1T-based TFT devices.

Film Morphology. Atomic force microscopy (AFM) measurements were taken for the same substrates which were fabricated for TFT devices. Figure 5 shows the AFM images of semiconducting layers that did not undergo any thermal treatments. These AFM images indicate significant morphological differences between PF-1T and PF-4T as

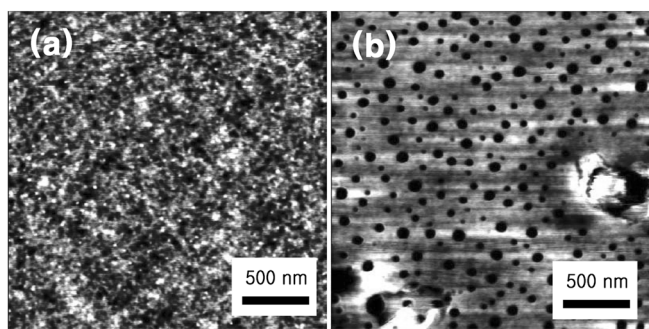


Figure 5. Atomic force microscopy images of PF-1T (a) and PF-4T (b).

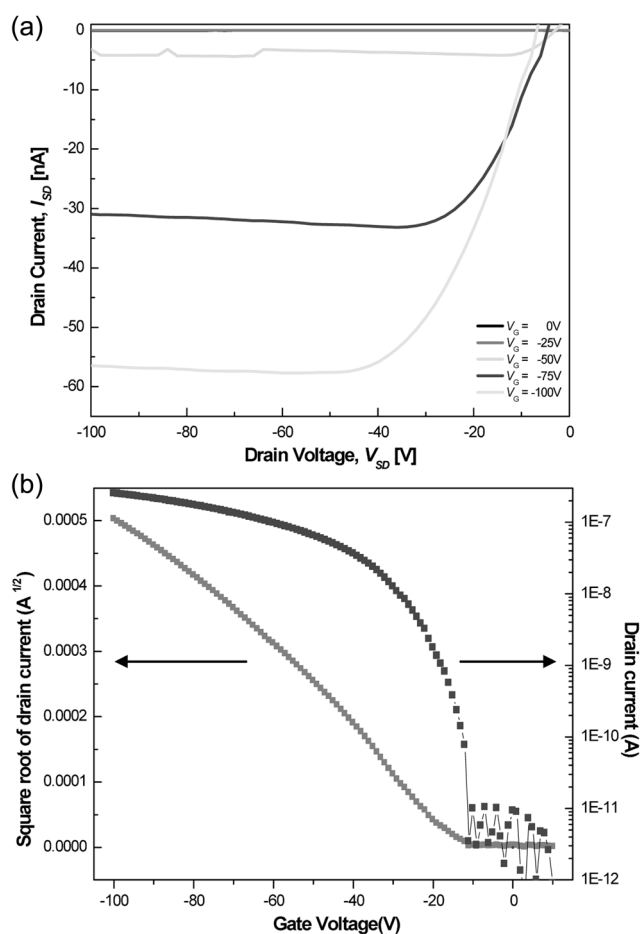


Figure 6. Electrical characteristics of PF-1T in air: (a) output characteristics and (b) transfer characteristics (drain-source voltage = -100 V).

films. PF-1T film has an isotropic nodule structure similar to high-MW P3HT.²³ Thus, the main backbone chains of PF-1T can interconnect ordered areas and prevent charge carriers from being trapped by the disordered boundary regions by creating a continuous pathway through the film. However, in the case of PF-4T, crystalline regions did not exist and numerous film defects such as pin holes were detected. These film defects and non-crystalline regions degraded the thin-film transistor (TFT) performance.

TFT Characteristics. The TFT properties of the polymers as a solution-processed thin-film semiconductor were

evaluated using a top-contact TFT configuration built on an n-doped silicon wafer. Figure 6 shows the typical output and transfer curves of a representative as-prepared TFT device under ambient conditions without taking any precautions to insulate the materials and devices from exposure to air, moisture, and light. The field-effect mobility was extracted from the following equation:²⁴

$$\text{Saturated regime } (V_D > V_G): I_D = (W/2L)\mu C_i (V_G - V_T)^2$$

where I_D is the drain current in the saturated region, W and L are the channel width and length, respectively, μ is the field-effect mobility, C_i is the capacitance per unit area of the gate dielectric layer, and V_G and V_T are the gate and threshold voltages, respectively. A thin film of PF-1T gave a saturation mobility of 0.001 – 0.003 $\text{cm}^2 \text{V}^{-1} \text{s}^{-1}$, an on/off ratio of 1.0×10^5 , and a small threshold voltage of -8.3 V. In the case of the PF-4T, the thin-film transistor mobility was 6×10^{-6} $\text{cm}^2 \text{V}^{-1} \text{s}^{-1}$. PF-4T was expected to have more effective conjugation length. However, the mobility of PF-1T was much higher than that of PF-4T because the former had much better crystalline regions due to the well ordered alignments of the molecular structure. When these alternating copolymers were synthesized, hexyl-thiophene derivatives randomly coupled with fluorene monomers regardless of the alkyl direction of thiophene derivatives. Therefore, due to the longer unit length of the thiophene derivatives of PF-4T compared to PF-1T, interchain alignment of PF-4T was twisted sterically. These results suggest that the relationship between the structures of semiconducting materials and their TFT device performances is very important. In addition, because of fluorene moieties in polymer backbones, TFT devices showed significantly low off-current. This can be attributed to the stable HOMO energy levels in these polymers, similar to the case of F8TT.²⁵

Conclusions

PF-1T and PF-4T copolymers were successfully synthesized through the palladium-catalyzed Suzuki coupling reaction. The synthesized polymers were found to exhibit good thermal stability, losing less than 5% of their weights on heating to about 400 °C, as determined with TGA. Cyclic voltammetry measurements showed that the two polymers have low HOMO levels, indicating high resistance against oxidative doping. AFM and XRD results showed that PF-1T has superior ordered regions because it has a lesser hindered structure than PF-4T. TFT devices were fabricated using the top contact geometry. TFT devices of PF-1T gave a mobility of 0.001 – 0.003 $\text{cm}^2 \text{V}^{-1} \text{s}^{-1}$, an on/off ratio of 1.0×10^5 , and a small threshold voltage of -8.3 V. In the case of PF-4T, the mobility was 6×10^{-6} $\text{cm}^2 \text{V}^{-1} \text{s}^{-1}$. These results suggest that molecular structures have significant impact on the TFT device performances.

Acknowledgments. This work was supported by a grant (F0004021-2007-23) from the Information Display R&D Center, one of the 21st Century Frontier R&D Program

funded by the Ministry of Commerce, Industry, and Energy of the Korean Government and by the Brain Korea 21 (BK21) project.

References

1. Burroughes, J. H.; Bradley, D. D. C.; Brown, A. R.; Marks, R. N.; Mackey, K.; Friend, R. H.; Burns, P. L.; Holmes, A. B. *Nature (London)* **1990**, *347*, 539.
2. Friend, R. H.; Gymer, R. W.; Holmes, A. B.; Burroughes, J. H.; Marks, R. N.; Taliani, C.; Bradley, D. D. C.; Dos Santos, D. A.; Brédas, J. L.; Lögdlund, M.; Salaneck, W. R. *Nature (London)* **1999**, *397*, 121.
3. Shim, H.-K.; Jin, J.-I. *Adv. Polym. Sci.* **2002**, *158*, 193.
4. Dimitrakopoulos, C.; Malenfant, P. *Adv. Mater.* **2002**, *14*, 99.
5. Katz, H.; Bao, Z. *J. Phys. Chem. B* **2000**, *104*, 671-678.
6. Horowitz, G. *J. Mater. Res.* **2004**, *19*, 1946-1962.
7. Schmidt-Mende, L.; Fechtenkötter, A.; Müllen, K.; Moons, E.; Friend, R. H.; MacKenzie, J. D. *Science* **2001**, *293*, 1119.
8. Brabec, C. J.; Sariciftci, N. S.; Hummelen, J. C. *Adv. Funct. Mater.* **2001**, *11*, 15.
9. Coakley, K. M.; McGehee, M. D. *Chem. Mater.* **2004**, *16*, 4533-4542.
10. Klauk, H.; Jackson, N. *Solid State Technol.* **2000**, *43*, 63.
11. Gelinck, G. H.; Geuns, T. C. T.; De Leeuw, D. M. *Appl. Phys. Lett.* **2000**, *77*, 1487.
12. Son, J.-H.; Kang, I.-N.; Oh, S.-Y.; Park, J.-W. *Bull. Korean Chem. Soc.* **2007**, *28*, 995-998.
13. Ong, B. S.; Wu, Y.; Liu, P.; Gardner, S. *J. Am. Chem. Soc.* **2004**, *126*, 3378-3379.
14. Kim, Y. M.; Lim, E.; Kang, I.-N.; Jung, B.-J.; Lee, J.; Koo, B. W.; Do, L.-M.; Shim, H.-K. *Macromolecules* **2006**, *39*, 4081-4085.
15. McCulloch, I.; Heeney, M.; Bailey, C.; Genevicius, K.; Macdonald, I.; Shkunov, M.; David, S.; Tierney, S.; Wagner, R.; Zhang, W.; Chabinyc, M. L.; Kline, R. J.; McGehee, M. D.; Toney, M. F. *Nature Materials* **2006**, *5*, 328.
16. Lim, E.; Jung, B.-J.; Shim, H.-K. *Macromolecules* **2003**, *35*, 4288.
17. Pommerehe, J.; Vestweber, H.; Guss, W.; Mahrt, R.; Bassler, H. H.; Porsch, M.; Daub, J. *Adv. Mater.* **1995**, *7*, 551-554.
18. Meng, H.; Zheng, J.; Lovinger, A. J.; Wang, B.-C.; Patten, P. G. V.; Bao, Z. *Chem. Mater.* **2003**, *15*, 1778-1787.
19. Grell, M.; Bradley, D. D. C.; Ungar, G.; Hill, J.; Whitehead, K. S. *Macromolecules* **1999**, *32*, 5810.
20. Kawana, S.; Durrell, M.; Lu, J.; Macdonald, J. E.; Grell, M.; Bradley, D. D. C.; Jukes, C.; Jones, R. A. L.; Bennett, S. L. *Polymer* **2002**, *43*, 1907.
21. Yamamoto, T.; Kokubo, H.; Morikita, T. *J. Polym. Sci., Part B: Polym. Phys.* **2001**, *39*, 1713.
22. Bao, Z.; Dodabalapur, A.; Lovinger, A. J. *Appl. Phys. Lett.* **1996**, *69*, 4108.
23. Kline, R. J.; McGehee, M. D.; Kadnikova, E. N.; Liu, J.; Frechet, J. M. J.; Toney, M. F. *Macromolecules* **2005**, *38*, 3312-3319.
24. Dimitrakopoulos, C. D.; Melenfant, P. R. L. *Adv. Mater.* **2002**, *14*, 99-117.
25. Lim, E.; Jung, B.-J.; Lee, J.; Shim, H.-K.; Lee, J.-I.; Yang, Y. S.; Do, L.-M. *Macromolecules* **2005**, *38*, 4531.